The Maintenance of an Equatorially Asymmetric State in a Hybrid Coupled GCM

SHANG-PING XIE

Program in Atmospheric and Oceanic Sciences, Princeton University, Princeton, New Jersey

(Manuscript received 9 August 1993, in final form 9 February 1994)

ABSTRACT

An ocean general circulation model is coupled with a simple atmosphere model to investigate the formation mechanism of the intertropical convergence zone in the eastern Pacific, which is observed in the Northern Hemisphere. The coupled model develops an asymmetric state under conditions symmetric about the equator. The zonal variation in equatorial upwelling leads to pronounced differences between the western and other parts of the ocean. In the western warm water pool region, where the cooling effect of the equatorial upwelling is suppressed, both atmospheric and oceanic surface conditions are symmetric about the equator. On the other hand, in the central region where the upwelling cools the equatorial ocean, a single ITCZ forms off the equator in the Northern or Southern Hemisphere, depending on the initial condition. A strong contrast exists in the sea surface temperature SST between the hemispheres; SST is much higher at the latitude of the ITCZ than that on the other side of the equator. This high SST is crucial for the development of deep convection in the ITCZ. An air–sea interaction mechanism, where the wind speed–dependent surface evaporation plays a crucial role, maintains the asymmetric state, confirming the results from a previous two-dimensional model study.

1. Introduction

Most of the absorption of solar radiation occurs at the surface of the earth. In tropical deep convection, water vapor condenses and latent heat is released. Since evaporation is driven by the solar radiation absorbed at the surface, it is not surprising to see tropical convective activity that is consistent with the solar radiation. Over the land, Indian, and western Pacific Oceans, it is indeed the case; deep convection in the intertropical convergence zone (ITCZ) follows the seasonal migration of the sun. In the eastern Pacific and Atlantic, peculiar behavior is observed from the satellite measurements; the ITCZ stays in the Northern Hemisphere throughout the year, even though the sun moves back and forth across the equator (Kornfield et al. 1967; Hubert et al. 1969; Mitchell and Wallace 1992). The location of the ITCZ has important consequences for the tropical climate. Its persistent stay in the Northern Hemisphere has been proposed as a cause of the annual cycle in the sea surface temperature (SST) in the eastern equatorial Pacific[1] (Xie 1994; K. Miyakoda 1994, personal communication). In addition, the interannual variation in the location of the ITCZ may have an effect on the evolution of the El Niño–Southern Oscillation (ENSO) (Philander et al. 1984).

Deep convection over the ocean is strongly influenced by the sea surface temperature distribution. In the eastern Pacific and Atlantic, a zonally oriented band of high SST is collocated with the ITCZ. From an atmospheric point of view, the reason for the northern ITCZ is the high SST, which leads to low moist static stability and deep convection (Manabe et al. 1974). The sensitivity of convection to the SST distribution is underlined by the fact that two ITCZs sometimes appear, one in each hemisphere, in the boreal spring when the equatorial ocean warms up and the equatorial asymmetry in the SST distribution diminishes (Kornfield et al. 1967; Hubert et al. 1969). From an oceanographic point of view, on the other hand, the SST is high presumably because the atmospheric convergence zone is there. Forced with observed winds, the ocean general circulation model (GCM) can reproduce the observed oceanic state with SST being high in the Northern and low in the Southern Hemisphere (Philander and Seigel 1985). The interdependence between deep convection and SST distribution indicates that the interaction between the ocean and atmosphere plays a key role in setting and maintaining this hemispheric asymmetry, although other factors such as landmass distribution may help the ocean–atmospheric system to choose the Northern Hemisphere to form its ITCZ.

A recent study by Xie and Philander (1994) provides a clue to this air–sea coupling problem. In a two-dimensional coupled ocean–atmosphere model that neglects zonal variations, they found equatorially asym-

Corresponding author address: Dr. Shang-Ping Xie, Joint Institute for the Study of the Atmosphere and Ocean, GJ-40, University of Washington, Seattle, WA 98195.

[1] On the equator, the solar radiation at the top of the atmosphere has virtually no annual component and is dominated by a semiannual cycle. Therefore, it cannot be the direct cause of the equatorial annual cycle in SST.

metric solutions with a single off-equatorial ITCZ and warm SST forming only in one hemisphere, even when the external conditions are perfectly symmetric. Air–sea coupling that involves vertical mixing in the ocean mixed layer and surface evaporation is crucial in their model to maintain such an asymmetric state. These interactions require a shallow thermocline and strong oceanic upwelling near the equator, consistent with the fact that the asymmetric ITCZ is observed in the Atlantic and eastern Pacific but not in the Indian and western Pacific Oceans.

This study extends Xie and Philander's work by using a three-dimensional model to include the zonal dimension. A three-dimensional ocean general circulation model (GCM) will be coupled with a simple atmospheric model to form a so-called hybrid coupled model (Neelin 1991). Following Xie and Philander, we will set our model to be symmetric about the equator to isolate air–sea interaction processes. The equatorially symmetric air–sea coupling modes, which are important for the development of ENSO, have been extensively investigated in previous studies (see Philander 1990; McCreary and Anderson 1991; Neelin et al. 1994 for reviews). The purpose of this study is to explore the possibility that an equatorially asymmetric mode might exist and be related to the observed northern ITCZ. We will examine the effect of zonal variation in the thermocline depth on the formation of the ITCZ. The effects of an asymmetric ITCZ on the oceanic currents and thermocline structures will also be studied.

The rest of the paper is organized as follows. Sections 2 and 3 describe the hybrid coupled model and coupling procedures. Sections 3 and 4 present results from the hybrid model experiments. Section 5 gives a summary.

2. Model

A linear reduced gravity model (phase speed 45 m s^{-1}) is used for the atmosphere (Matsuno 1966; Gill 1980). The model atmosphere is forced by cumulus heating that occurs only when SST exceeds a criterion $Tc = 27.5$°C (Graham and Barnett 1987). We parameterize cumulus heating as a function of SST

$$\frac{Q(T)}{K_Q} = \begin{cases} 0, & T < 27.5 \\ T - 27.5, & T > 27.5. \end{cases} \quad (2.1)$$

Good correlation between high SST and high convective activity is found in the observations and in GCM experiments (Manabe et al. 1974). Sidestepping the complicated problem of how this correlation is established, the parameterization of (2.1) enables us to explore the air–sea interaction in a relatively simple system. Equation (2.1) has been previously used by Anderson and McCreary (1985) and Xie et al. (1989) in their ENSO studies. The atmospheric model is solved in a global domain by using the spectral method and is truncated rhomboidally at zonal wavenumber 63. The zonal and meridional resolutions are 2° and 1°, respectively. Second-order viscosity and diffusion terms are included in the momentum and temperature equations, respectively, with coefficients of 10^5 m^2 s^{-1}. The Rayleigh and Newtonian damping rates are $(2 \text{ days})^{-1}$ and the coupling coefficient is $K_Q = 2.4 \times 10^{-3}$ m^2 s^{-3} K^{-1}.

We use the Geophysical Fluid Dynamics Laboratory (GFDL) Modular Ocean Model (MOM), described by Bryan (1969) and Pacanowski et al. (1990). It has been applied to the Tropics to study ENSO (Philander and Siegel 1985) and the seasonal cycle (Philander et al. 1987; Koeberle and Philander 1994). The GCM has also previously been coupled to a simple atmospheric model to study ENSO cycles (Neelin 1990). The salinity is not calculated and is fixed at 35 psu (practical salinity unit) in the present study. The model has a rectangular configuration that extends from 40°S to 40°N and 130°E to 80°W; it resembles the Pacific Ocean. The model is 3000 m deep and has 15 vertical levels with 9 of them in the upper 300 m. The Richardson number–dependent, implicit vertical mixing scheme is used as in Pacanowski and Philander (1981). Lateral viscosity and diffusivity coefficients are 4×10^3 and 2×10^3 m^2 s^{-1}, respectively. The longitudinal and meridional resolutions are 3° and 1° throughout the domain. A time step of 1 hour is used. In the so-called buffer zones poleward of 30°, a Newtonian cooling is applied to relax the temperature toward hemispherically and zonally averaged climatology constructed from the Levitus dataset (Levitus 1982). The coefficient of the Newtonian cooling increases from zero at 31° to $(5 \text{ days})^{-1}$ at the poleward boundaries. Rayleigh friction with the same coefficient is applied to momentum equations, which relaxes the current velocity toward zero. To assure that the winds in the buffer zone are compatible with the ocean thermal structure, we apply annual, zonal, and hemispheric-mean COADS winds in the buffer zone. Between 20° and 30°, winds obtained from the atmospheric model are gradually changed to the COADS winds at 30°. Equatorward of 20° winds obtained from Gill's model are applied. To resolve the western boundary current with the coarse zonal resolution, the viscosity coefficient is linearly increased from 148°E toward the western boundary, where it is 4×10^4 m^2 s^{-1}.

The ocean is driven by wind stress and surface heat flux. The surface heat flux consists of four components: shortwave and longwave radiation, and sensible and latent heat. Shortwave radiation is calculated using Reed's (1977) formula and longwave calculation follows Budyko (1974) (see Rosati and Miyakota 1988 for details). A constant albedo of 0.15 is used, which is somewhat too large but necessary in order for the SST to have reasonable values in the western Pacific. Cloudiness C is assumed to be a simple function of latitude φ

$$C = 0.5 + 0.25(\varphi/40°)^2.$$

Sensible and latent heat fluxes are calculated by using bulk formulas. Over the tropical oceans, the latent heat flux is an order of magnitude larger than the sensible heat and hence roughly balances the net radiative heat flux in the absence of the ocean dynamic effects. The formula for latent heat flux is

$$Q_E = \rho_a C_E |U| [q(T_s) - \mathrm{RH} q(T_a)], \quad (2.2)$$

where T_a is the air temperature, q is the saturated moisture content, and RH the relative humidity. When the wind speed is less than 4.8 m s^{-1}, the value of $|U|$ in (2.3) is set to 4.8 m s^{-1}, mimicking the effect of high-frequency atmospheric disturbances (Philander and Siegel 1985). Exchange coefficients for latent and sensible heats have the same values, $C_E = C_H = 1.4 \times 10^{-3}$. A smaller value for momentum ($C_D = 1.0 \times 10^{-3}$) is used. A larger value of C_D leads to an equatorial cold tongue too strong in a simulation forced with COADS surface winds (not shown). The relative humidity is specified as a simple function of latitude

$$\mathrm{RH} = 0.75 + 0.05 \cos(\pi\varphi/30°),$$

which has a minimum in the subtropics. Deep convection affects distributions of both the cloud cover and the relative humidity. These two effects of deep convection counteract each other on SST. The high cloudiness at the ITCZ acts to dampen the equatorial asymmetry in SST, while the collocated high relative humidity hampers surface evaporation and acts to enhance the SST asymmetry. For simplicity, both the cloudiness and relative humidity are fixed in time and are symmetric about the equator in this study. Their net effect on SST needs to be assessed in future studies.

3. Couplings

Our strategy is to first construct an equatorially symmetric basic state and to see if the coupled model develops an asymmetric state by itself.

The basic-state winds of the atmosphere are based on the COADS (Comprehensive Ocean–Atmospheric Data Set), and the land grids are filled in the following way. At latitudes where the North American continent falls inside the model domain, we shift the COADS data east of the central longitude ($\lambda = 205°$ or 155°W) eastward so that the first COADS land grid is on the eastern boundary of the rectangular model ocean. This fills the land grids but leaves a blank area east of $\lambda = 205°$. Since the winds in the center of the Pacific change very little in the zonal direction, this blank area is filled with the data at $\lambda = 205°$. In other words, for $\Delta\lambda > 0$,

$$U(\lambda) = \begin{cases} U(\lambda - \Delta\lambda), & \text{if} \quad \lambda > 205 - \Delta\lambda \\ U(205), & \text{if} \quad 205 \leqslant \lambda \leqslant 205 - \Delta\lambda, \end{cases}$$

where λ is longitude in degrees, λ_L is the longitude of the first COADS land point, and $\Delta\lambda = 280 - \lambda_L$. The same procedure is applied to fill the data in other land grids. This procedure preserves the zonal scale of the atmospheric response to the land–sea contrast such as the high center off the west coast of North America. The wind data are then averaged between the hemispheres. The resultant field is shown in Fig. 1a. Easterly trades prevail in the Tropics. In the western Pacific, there is a surface wind convergence zone corresponding to the convection center there. In addition, two off-equatorial ITCZs are located around 7° in the central and eastern parts of the ocean, a result of hemispheric averaging. The winds are divergent in the equatorial region sandwiched by the ITCZs. Over the eastern equatorial region the observed strong southerlies are averaged out, and the winds are very weak in Fig. 1a.

Using the winds in Fig. 1a and imposing hemispherically averaged surface air temperatures, we drive the ocean model for five years. The model SST field at the end of the fifth year is shown in Fig. 1b. It resembles the hemispherically averaged COADS SST field, except in the coastal region off the eastern boundary where we used an idealized coastal line. The warm water pool in the western and the equatorial cold tongue in the central and eastern oceans are well reproduced. The SST maximum occurs off the equator in most of the domain. The SST along the line of maximum SST ($T_y = 0$) is high in the west and low in the east, primarily due to the variation in the imposed surface air temperature.

In the following experiments, only wind and SST anomalies from the basic states shown in Fig. 1 are coupled. When an SST deviation from the basic-state SST field occurs, the anomalous heating to the atmosphere is calculated by $Q' = Q(T_S) - Q(T_{s0})$, where $Q(T)$ is given in (2.1); T_s and T_{s0} are model and basic-state SSTs. The heating anomaly is then used to drive Gill's model and obtain an anomalous wind field. The wind anomalies are added to the external winds shown in Fig. 1a to form the surface boundary condition for the ocean. This anomaly coupling method has been previously used in various coupled models (Schopf and Suarez 1988; Xie et al. 1989; Neelin 1990). Note that in this model, surface winds not only drive ocean currents but also affect the SST by modifying surface heat fluxes. Since the change in the surface air temperature Ta is mainly caused by that in SST, the air–sea temperature difference is assumed to be constant in time; that is, $T_S - T_a = (T_{s0} - T_{a0})$ where T_{a0} is the hemispheric average of the COADS air temperature. The atmosphere and ocean are coupled once a day. In the following experiments, the solar radiation is fixed at its annual mean value and is symmetric about the equator.

4. Standard run

The steady state of the ocean model driven by the basic state wind is a possible solution for the coupled

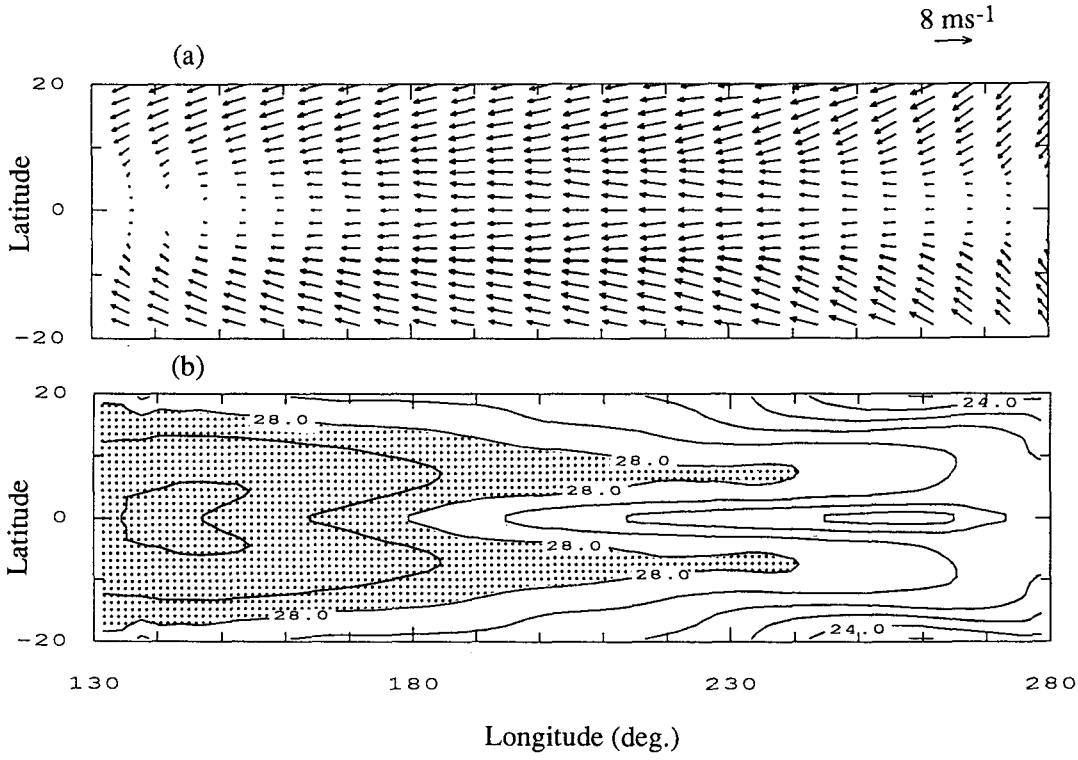

FIG. 1. Horizontal distributions of (a) surface winds (scale shown in the upper-right corner) and (b) SST (contour interval: 1°C) in the basic state. Area with SST higher than 28°C is shaded.

system. We perturb this solution by imposing southerly winds of a constant speed 3 m s^{-1} temporally for one month everywhere in the model domain; these winds cause an equatorial asymmetry (Philander and Pacanowski 1981). The additional southerlies are then turned off and the coupled model is let free to run for

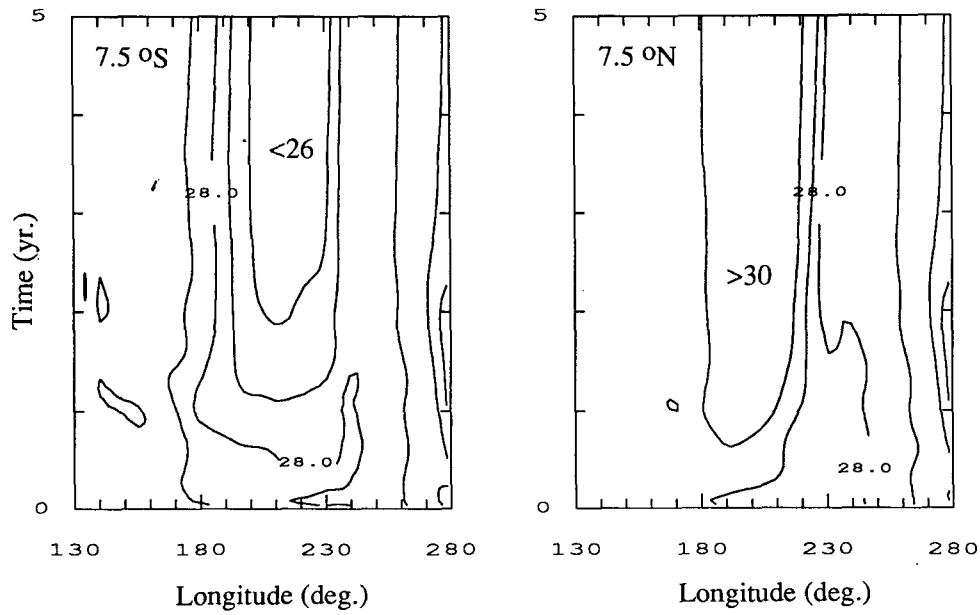

FIG. 2. Time–longitude sections of SST at (a) 7.5°S and (b) 7.5°N (contour interval: 1°C).

15 years. Figure 2 depicts the longitude–time evolution of the model SST at 7.5°N and 7.5°S for the first five years. In both western and eastern parts of the ocean, there is little SST change. In the central part, on the other hand, an equatorial asymmetry is built up. The SST decreases rapidly at 7.5°S but increases slightly at 7.5°N for the first two years. After this, the SST field approaches a steady state.

Model surface fields averaged over the last two model years are shown in Fig. 3. An equatorial antisymmetric pattern dominates the field of cumulus heating anomaly (Fig. 3a). Positive and negative heating anomalies are found north and south of the equator, respectively. In response, southwesterly anomalies are generated between the northerly positive heating center and the equator (Fig. 3b). As a result, trade winds weaken (Fig. 3c). South of the equator, on the other hand, southeasterly anomalies are present, strengthening the easterly trades.

Figure 3d depicts the horizontal distribution of SST. In the western Pacific where the cooling effect of equatorial upwelling is weak, the SST is higher at the equator than that off the equator, since the solar radiation is maximum at the equator. The ITCZ then sits on the equator if it follows the SST maximum as in the present model. As a result, the SST is nearly symmetric about the equator. In the central ocean, on the other hand, the thermocline is shallow and the cooling by the equatorial upwelling is so strong that the SST at the equator is too low to support the deep convection. The ITCZ

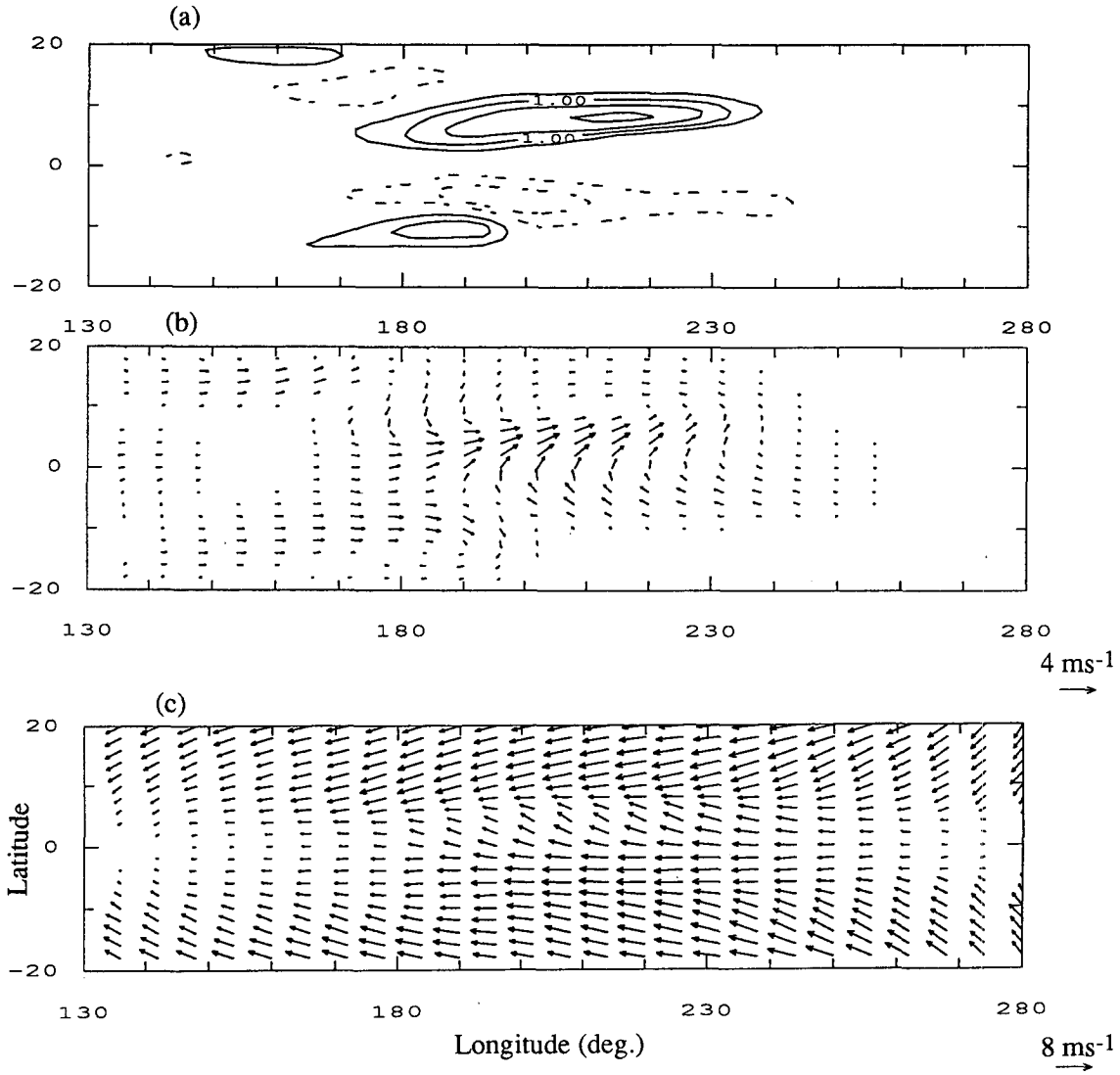

FIG. 3. Horizontal distributions of (a) anomalous heating to the atmosphere (Q/K_Q; contour interval: 0.5 K; negative in dashed line and zero contour omitted), (b) anomalous and (c) total wind velocity, (d) SST (contour interval: 1°C; shaded if SST $\geq$ 28°C), and (e) surface current velocity.

then has to form in an off-equatorial region. Under this circumstance, the air–sea interaction selects one of the hemispheres to form the ITCZ, while suppressing the deep convection in the other by decreasing the SST there. In the central part of the domain, the SST field exhibits a strong asymmetry and the off-equatorial maximum to the north of the equator is a few degrees higher than that to the south. East of $\lambda = 200°$ (or 160°W), areas of SST higher than 27.5°C, which corresponds to the model ITCZ, are found only in the Northern Hemisphere. This is consistent with the finding of Xie and Philander (1994) in a two-dimensional coupled model that strong equatorial upwelling is necessary for the asymmetric state to develop.

An SST–wind feedback is responsible for this equatorially asymmetric state. Figure 4a gives meridional profiles of surface wind speed and SST, which are nearly out of phase. The low winds near the SST maximum in the Northern Hemisphere are due to the weakening of easterly trades. The latter is associated with the southerly cross-equatorial winds that converge onto the ITCZ. Through surface latent heat flux, winds can affect SST. Latent heat flux is the major component of surface heat flux that balances the solar radiation. Due to equatorially symmetric solar radiation, both net surface heat flux and its latent heat component are to a large degree symmetric in the model (Fig. 4b) and in the observations (Weare et al. 1981; Esbensen and Kushnir 1981; Oberhuber 1988). With an equatorially symmetric distribution of latent heat flux, an asymmetric wind speed distribution can lead to an asymmetry in SST. Because of the low wind speeds, the SST to the north of the equator has to be high to supply latent heat that offsets the downward radiation flux. On the other hand, since the winds are high to the south of the equator, a low SST is enough to give out the same amount of latent heat. To be more quantitative, we compare the surface conditions at 7.5°N, where the SST reaches maximum, and 7.5°S. Since the latent heat fluxes are nearly equal at the two latitudes, we have $U_N q(T_N) = U_S q(T_S)$ with subscripts N and S denoting 7.5°N and 7.5°S. From Fig. 4a, $T_N = 30.5°C$ and $U_S/U_N = 1.3$. By using the Clausius–Clapeyron equation and $T_S = q^{-1}(U_S/U_N q(T_N))$, we obtain $T_S = 26.0°C$, in a good agreement with our GCM calculation. We will demonstrate the importance of this SST (evaporation)–wind mechanism in a more explicit way in the next section.

The model SST field west of 240° resembles the observed field in the Pacific, having such observed features as the equatorial cold tongue and the high SST band in the Northern Hemisphere. In the eastern part of the model domain, however, the SST is quite equatorially symmetric for the following reasons. First, when the eastern boundary is approached, the surface wind field is more and more dominated by the equatorially symmetric Kelvin wave response to an oceanic heating, whether the heating is symmetric or asymmetric. Second, the basic-state winds in the eastern equatorial region are much weaker than 4.8 m s^{-1}, the

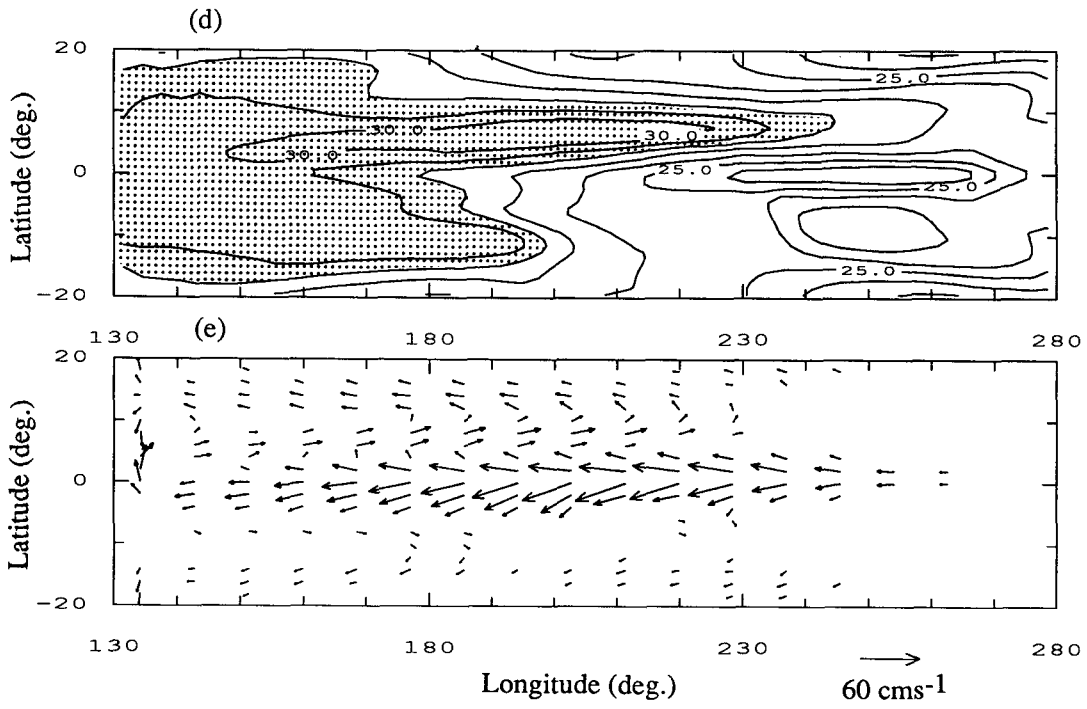

FIG. 3. (*Continued*)

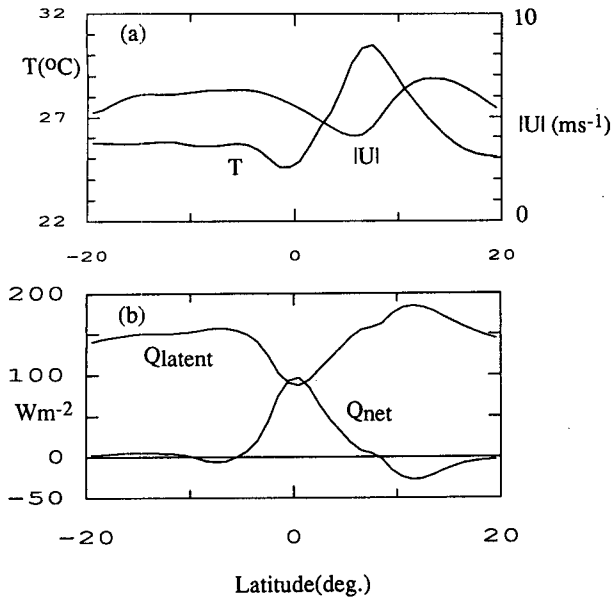

FIG. 4. (a) Surface wind speed and SST and (b) net surface heat flux and its latent heat component as functions of latitude at 140°W.

minimum wind speed for evaporation calculation. Therefore, an anomalous wind does not feed back onto the SST anomaly through evaporation. These deficiencies of the atmospheric model should be improved in future studies. Including the SST gradient forcing in the atmospheric boundary layer (Lindzen and Nigam 1987) may improve the model performance in the east by enhancing the coupling between the ocean and atmosphere.

The major tropical surface currents are reproduced in the model (Fig. 3e). South of the northerly SST maximum or the ITCZ, there is the westward South Equatorial Current with a speed as high as 0.5 m s^{-1}. North of the ITCZ is the North Equatorial Current. Between these two westward currents, a countercurrent flows eastward roughly along the line of $T_y = 0$. This North Equatorial Countercurrent does not penetrate eastward enough to hit the eastern boundary, in contrast to the observations. One might attribute the cause of the warm water SST band in the Northern Hemisphere to the eastward countercurrent, which could bring warm water from the west. However, this seems not to be the case, since the countercurrent is not purely zonal but has a northward component due to the Ekman drift. Therefore, a water particle, starting from the western ocean with high temperature and riding on the countercurrent, may not move far enough to the east to establish the warm band across the basin. The water in the high SST band in the central part of the ocean may actually come from somewhere in the equatorial cold tongue.

Figure 5 shows the meridional sections of ocean temperature and zonal velocity along 140°W ($\lambda = 220°$). The equatorial upwelling is manifested by the shallow thermocline and cold mixed layer water. Near the equator, there is an equatorial undercurrent below the westward flow at the surface. Coinciding with the warm SST region, a ridge in the thermocline depth is found north of the equator, maintained by the curl of the zonal wind that is associated with the ITCZ. A North Equatorial Countercurrent with a speed of 0.1 m s^{-1} exists south of the ridge. There is another much weaker ridge in thermocline depth south of the equator, an artifact caused by the hemispheric averaging of COADS winds. Although also seen in the thermocline, the equatorial asymmetry in ocean temperature is most evident in the mixed layer. There is a sharp front north of the equator, and the mixed layer temperature increases northward rapidly from the equator. To the south of the equator, on the other hand, the mixed layer temperatures are much colder than those in the Northern Hemisphere.

In the two-dimensional model the equatorially symmetric solution with a double ITCZ is stable to infinitesimal disturbances (Xie and Philander 1994). In con-

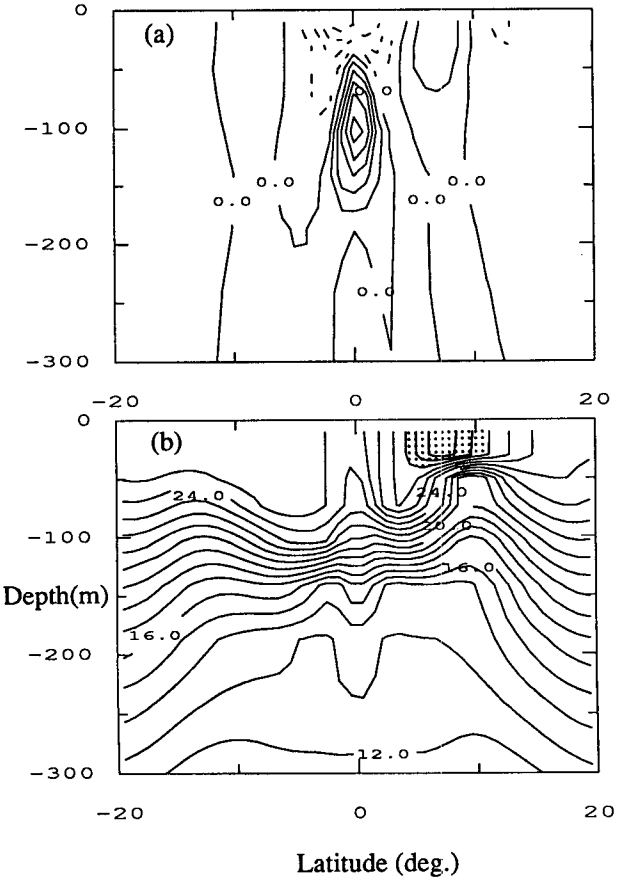

FIG. 5. Latitude–depth sections of (a) zonal current velocity (contour interval: 0.1 m s^{-1}; negative in dashed line) and (b) ocean temperature (contour interval: 1°C; shaded if $T \geq 28°C$) along 140°W.

trast, the symmetric state seems unstable to machine round-off errors in this three-dimensional hybrid GCM. In an experiment with the symmetric basic state in Fig. 1b as the initial condition, the model develops an equatorial asymmetry due to the small round-off errors and finally settles into the asymmetric solution with the ITCZ in the Southern Hemisphere in about 10 years. This difference may be due to the three-dimensionality and/or to the difference in ocean dynamics between the two models.

5. Symmetric dynamics run

In the present model there are two ways for the atmosphere to affect the ocean: through the wind stress and evaporation. The phase relation between the SST and surface wind speed in the standard run suggests that evaporation maintains the equatorial asymmetry in the SST distribution. To demonstrate this explicitly, we eliminate the asymmetry in ocean dynamics by artificially averaging the wind stress between the hemispheres before applying it to the ocean. At the same time, we use the wind speed for evaporation calculation as it is from the atmospheric model. Although the difference in evaporation may cause a little equatorial asymmetry in vertical mixing and thus in the ocean dynamic fields, we will call this experiment the symmetric dynamics run.

An asymmetric solution is obtained from this symmetric dynamics run, whose horizontal structures are shown in Fig. 6. An antisymmetric heating anomaly pattern similar to that in the standard run appears. As a result, the trades weaken to the south and intensify to the north of the equator. The SST field is very similar to that in Fig. 3d except that it becomes more symmetric about the equator in the western part of the ocean. This suggests that the weak asymmetry in the western ocean in the standard run is caused by the ocean dynamic effects.

Figure 7 depicts the meridional sections along 140°W. The effect of surface evaporation is only confined to the mixed layer where large temperature differences are seen between the Northern and Southern Hemispheres. The evaporation distribution itself, however, is nearly symmetric about the equator as in the standard run (not shown). The thermal structure of the ocean is almost symmetric below 50-m depth due to the symmetric wind stress forcing. As a result, the ocean current field is nearly symmetric at all depths.

This experiment illustrates that the interaction between the wind speed and SST through evaporation is essential in maintaining the asymmetric state. We have also performed an experiment opposite to the above, in which the wind speed for the evaporation calculation is hemispherically averaged but the wind stress to drive the ocean current is kept as it is from the atmospheric model. Eliminating the evaporation–wind feedback, this experiment tests the role of the ocean dynamics in maintaining an equatorially asymmetric state. Starting from the asymmetric solution of the standard model, the modified model falls into a symmetric steady state after about 10 years. This indicates that the ocean dynamic processes alone are not sufficient to maintain the equatorial asymmetry, reinforcing the importance of the evaporation–wind feedback.

6. Discussion

An ocean GCM has been coupled with Gill's atmosphere model to study the maintenance of the northerly ITCZ that is observed in the eastern Pacific. Under external conditions that are symmetric about the equator, the coupled model develops an asymmetric solution, confirming the results from the previous two-dimensional model. Over the western warm water pool region, both SST and atmospheric heating are symmetric about the equator, in response to the symmetric solar radiation forcing. In the central part of the ocean where the equatorial cold tongue develops due to upwelling, both SST and surface wind fields are asymmetric about the equator. A high SST band develops north of the equator, causing deep convection that forms the ITCZ. The weak winds at the location of the ITCZ, on the other hand, are responsible for the high SST there through latent heat flux. The cooling by equatorial upwelling, suppressing the deep convection and making the equator an impossible location for the ITCZ, is essential for the development of such an asymmetric state as in the two-dimensional model.

The present study demonstrates that the interaction between the surface wind and SST through evaporation is capable of maintaining an asymmetric ITCZ complex that consists of an atmospheric convergence zone and a collocated, zonally oriented high SST band. A different kind of evaporation–wind feedback operates in the tropical intraseasonal oscillations with a timescale from 30 to 60 days (Neelin et al. 1987; Xie et al. 1993). On this timescale, the SST does not change very much because of the large heat content of the upper ocean. As a result, high winds induce large surface evaporation that fuels deep convection. In contrast to the evaporation–wind feedback in the transient intraseasonal oscillations, it operates differently in the present steady-state problem of the ITCZ; high wind speeds do not lead to high evaporation but to low SST. This is because in a steady state, the rate of evaporation is not determined by the wind speed; instead, the latent heat flux is controlled by solar radiation and oceanic upwelling, features that are symmetric about the equator. For a given evaporation rate, high wind speeds decrease SST and vice versa.

The seasonal movement of the sun acts to destabilize the equatorially asymmetric solutions. For the solution with the ITCZ in the Northern Hemisphere, the solar radiation in the boreal fall, which is stronger in the

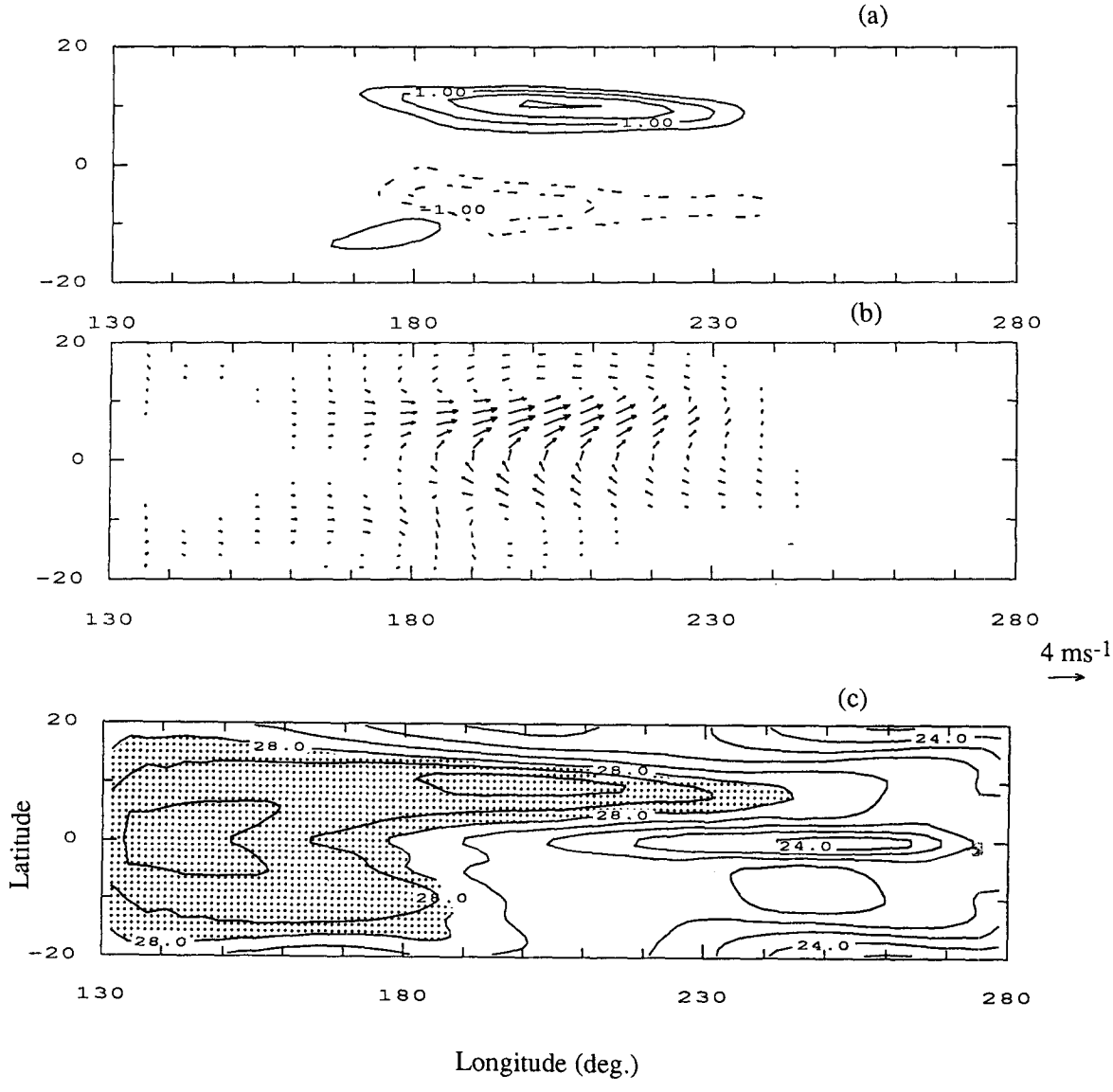

FIG. 6. Horizontal distributions of (a) anomalous heating to the atmosphere (Q/K_Q; contour interval: 0.5 K; negative in dashed line and zero contour omitted), (b) anomalous wind velocity, and (c) SST (contour interval: 1°C; shaded if SST $\geq$ 28°C) in the symmetric dynamics run.

Southern Hemisphere, acts to warm the SST to the south of the equator and hence to pull the ITCZ into the Southern Hemisphere. Since an equatorially asymmetric solution is stable to infinitesimal disturbances, one could expect the ITCZ to persist in the Northern Hemisphere at least under small annual variations in solar forcing.

This evaporation–wind feedback mechanism may best work in the interior ocean as in this hybrid model. It is highly possible that the maintenance of the asymmetric ITCZ differs from the coastal to interior regions. In the eastern region close to the coast, coastal upwelling seems to be the dominant process responsible for the cold SST south of the equator. Near the American continent strong southerly winds are observed, which flow along the coast of the continent and cause coastal upwelling. Lacking both land and topographic effects, Gill's model failed to produce such southerlies in the eastern coastal region. To improve the results in this region, a more realistic atmospheric model is needed. Because the external conditions are equatorially symmetric, a solution with a Southern Hemisphere ITCZ is also possible. In nature, the asymmetric land and topography distributions may play a key role in selecting the Northern Hemisphere mode.

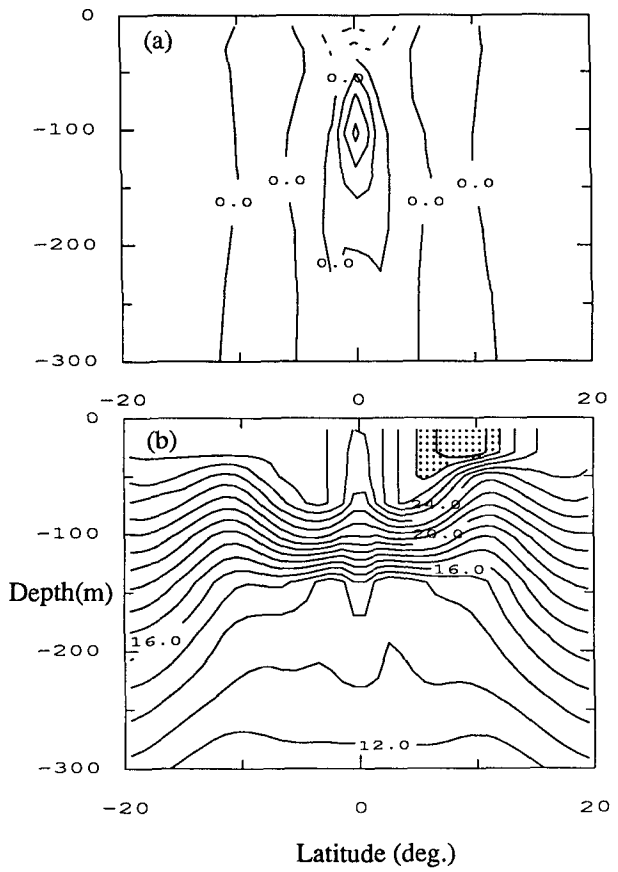

FIG. 7. Same as Fig. 5 but for the symmetric dynamics run.

In addition to the evaporation mechanism verified in this study, vertical mixing in the ocean mixed layer is another possible mechanism as discussed in Xie and Philander (1994), since its strength is also dependent on the wind speed. This mechanism is technically difficult to test in the present model where the mixing is related to the vertical shear of large-scale current and is thus affected by the wind stress. Future ocean turbulence measurements in off-equatorial regions could provide the meridional distribution of vertical mixing intensity and reveal its dependence on the wind speed.

The solution symmetric about the equator is unstable in this hybrid GCM. The transition from the symmetric to the asymmetric solutions involves an antisymmetric mode. This model, however, did not generate ENSO-like variability, possibly due to the change in the basic state to which the ENSO-related coupled instabilities are sensitive. Previous simple and intermediate air–sea coupling models have helped us to gain much insight into the coupled instabilities and ENSO. However, they treat the latent heat flux as a passive Newtonian cooling term and do not include the evaporation–wind feedback that is responsible for the asymmetric climatological mean state. It would be interesting to include this feedback mechanism in these models and examine the impact of a self-developed asymmetric mean state on the symmetric coupled instabilities. In the warm phase of the ENSO, the equator warms up so that the ITCZ moves southward. Whether this southward movement of the ITCZ has an effect on the El Niño, and the problem of the interaction between the ENSO and ITCZ in general, are interesting subjects of future study.

Acknowledgments. I would like to thank G. Philander and I. Held for their advice and stimulating discussion, and C. Koeberle for her assistance in setting up the MOM. Comments by N. Mantua and two anonymous referees were helpful in improving the manuscript. During the course of this study, which is funded by a grant from the National Oceanic and Atmospheric Administration (NA26G0102-01), I had the benefit of access to the GFDL computer resources. The views expressed herein are those of the author and do not necessarily reflect the views of NOAA or any of its agencies.

REFERENCES

Anderson, D. L. T., and J. P. McCreary, 1985: Slowly propagating disturbances in a coupled ocean–atmosphere model. *J. Atmos. Sci.*, **42,** 615–929.

Bryan, K., 1969: A numerical method for the study of the circulation of the World Ocean. *J. Comput. Phys.*, **4,** 347–376.

Budyko, M. S., 1974: *Climate and Life.* Academic Press, 508 pp.

Esbensen, S. K., and V. Kushnir, 1981: The heat budget of the global Ocean: An atlas based on estimates from surface marine observations. Rep. 29, Clim. Res. Inst., Oregon State University, Corvallis, OR, 27 pp., 188 figs.

Gill, A. E., 1980: Some simple solutions for heat-induced tropical circulation. *Quart. J. Roy. Meteor. Soc.*, **106,** 447–462.

Graham, N. E., and T. P. Barnett, 1987: Sea surface temperature, surface wind divergence and convection over tropical oceans. *Science,* **238,** 657–659.

Hubert, L. F., A. F. Krueger, and J. S. Winston, 1969: The double intertropical convergence zone—Fact or fiction? *J. Atmos. Sci.*, **26,** 771–773.

Koeberle, C., and S. G. H. Philander, 1994: On the processes that control seasonal variations of sea surface temperatures in the tropical Pacific Ocean. *Tellus,* **46A,** in press.

Kornfield, J., A. F. Hasler, K. J. Hanson, and V. E. Suomi, 1967: Photographic cloud climatology from ESSA III and V computer produced mosaics. *Bull. Amer. Meteor. Soc.*, **48,** 878–882.

Levitus, S., 1982: *Climatological Atlas of the World Ocean.* NOAA Prof. Paper No. 13, U.S. Govt. Printing Office, Washington, DC, 173 pp.

Lindzen, R. S., and S. Nigam, 1987: On the role of sea surface temperature gradients in forcing low-level winds and convergence in the tropics. *J. Atmos. Sci.*, **44,** 2418–2436.

Manabe, S., D. G. Hahn, and J. L. Holloway Jr., 1974: The seasonal variation of the tropical circulation as simulated by a global model of the atmosphere. *J. Atmos. Sci.*, **31,** 43–83.

Matsuno, T., 1966: Quasi-geostrophic motions in the equatorial area. *J. Meteor. Soc. Japan,* **44,** 25–43.

McCreary, J. P., and D. L. T. Anderson, 1991: An overview of coupled ocean-atmosphere models of El Niño and the Southern Oscillation. *J. Geophys. Res.*, **96,** 3125–3150.

Mitchell, T. P., and J. M. Wallace, 1992: The annual cycle in equatorial convection and sea surface temperature. *J. Climate,* **5,** 1140–1156.

Neelin, J. D., 1990: A hybrid coupled general circulation model for El Nino studies. *J. Atmos. Sci.*, **47,** 674–693.

——, I. M. Held, 1987: Evaporation-wind feedback and low-frequency variability in the tropical atmosphere. *J. Atmos. Sci.*, **44,** 2341–2348.

——, M. Latif, and F.-F. Jin, 1994: Dynamics of coupled ocean–atmosphere models: The tropical problem. *Ann. Rev. Fluid Mech.*, **26,** in press.

Oberhuber, J. M., 1988: An Atlas based on the "COADS" data set: The budgets of heat, buoyancy and turbulent kinetic energy at the surface of the global ocean. Report No. 15, Max-Planck-Institut fur Meteor., Hamburg, Germany, 20 pp. + figs.

Pacanowski, R. C., and S. G. H. Philander, 1981: Parameterization of vertical mixing in numerical models of tropical oceans. *J. Phys. Oceanogr.*, **11,** 1443–1451.

——, K. Dixon, and A. Rosati, 1990: GFDL Modular Ocean Model, GFDL Ocean Group Tech. Rep. No. 2, GFDL, Princeton, NJ, 46 pp.

Philander, S. G. H., 1990: *El Niño, La Niña, and the Southern Oscillation.* Academic Press, 293 pp.

—— and A. D. Seigel, 1985: Simulation of El Niño of 1982–1983. *Coupled Ocean–Atmosphere Models,* J. C. J. Nihoul, Ed., Elsevier Oceanogr. Series, 40, Elsevier, 517–541.

——, T. Yamagata, and R. C. Pacanowski, 1984: Unstable air–sea interactions in the tropics. *J. Atmos. Sci.*, **41,** 604–613.

——, W. J. Hurlin, and A. D. Seigel, 1987: Simulation of the seasonal cycle of the tropical Pacific Ocean. *J. Phys. Oceanogr.*, **17,** 1986–2002.

Rosati, A., and K. Miyakada, 1988: A general circulation model for upper ocean simulation. *J. Phys. Oceanogr.*, **18,** 1601–1626.

Reed, R. K., 1977: On estimating insolation over the ocean. *J. Phys. Oceanogr.*, **7,** 482–485.

Schopf, P. S., and M. J. Suarez, 1988: Vacillations in a coupled ocean–atmosphere model. *J. Atmos. Sci.*, **44,** 549–566.

Weare, B. C., P. T. Strub, and M. D. Samuel, 1981: Annual mean surface heat fluxes in the tropical Pacific Ocean. *J. Phys. Oceanogr.*, **11,** 705–717.

Xie, S.-P., 1994: On the genesis of the equatorial annual cycle. *J. Climate,* **7,** in press.

——, and S. G. H. Philander, 1994: A coupled ocean-atmosphere model of relevance to the ITCZ in the eastern Pacific. *Tellus,* **46A,** in press.

——, A. Kubokawa, and K. Hanawa, 1989: Oscillations with two feedback processes in a coupled ocean–atmosphere model. *J. Climate,* **2,** 946–964.

——, ——, and ——, 1993: Evaporation–wind feedback and the organizing of tropical convection on the planetary scale. Part I: Quasi-linear instability. *J. Atmos. Sci.*, **44,** 3873–3883.